

be summarized in the following key features: (1) **Coarse-to-Fine Tasks**: We systematically deconstruct image generation into four task categories: No-ref/Ref Image Creating/Editing, based on the presence or absence of source images and reference images. And further decompose them into 31 fine-grained tasks covering a broad spectrum of image generation requirements, culminating in a comprehensive benchmark. (2) **Multi-dimensional Metrics**: The evaluation framework assesses image generation capabilities across 6 dimensions: aesthetic quality, imaging quality, prompt following, source consistency, reference consistency, and controllability. 11 metrics are introduced to support the multi-dimensional evaluation. Notably, we introduce VLLM-QA, an innovative metric designed to assess the success of image editing by leveraging large models. (3) **Hybrid Data**: The data comes from real scenes and virtual generation, which effectively improves data diversity and alleviates the bias problem in model evaluation. Through ICE-Bench, we conduct a thorough analysis of existing generation models, revealing both the challenging nature of our benchmark and the gap between current model capabilities and real-world generation requirements. To foster further advancements in the field, we will open-source ICE-Bench, including its dataset, evaluation code, and models, thereby providing a valuable resource for the research community. The detail of ICE-Bench can be found at <https://ali-vilab.github.io/ICE-Bench-Page/>

1. Introduction

Image generation has witnessed remarkable advancements in recent years, driven by significant technological breakthroughs such as VAEs [17, 24, 49], GANs [16], and Diffusion Models [21, 27, 28, 39]. Image generation encompasses a broad array of tasks aimed at producing high-quality images that satisfy multiple criteria, including aesthetic appeal, imaging quality, and adherence to the given description, among others. Image generation tasks are boundless, owing to the wide range of conditions and the intricate nature of natural language-based instructions.

Existing image generation foundational models [2, 4, 15, 25, 33, 35, 46] predominantly focus on text-to-image creating, which aims to generate images based on textual descriptions. When addressing more complex tasks, most existing methods [3, 11, 22, 30, 32, 47, 55, 58] opt for minor architecture adjustments to the text-to-image foundational model, followed by parameter fine-tuning to tackle the specific task. Recently, efforts have been made to develop unified architectures capable of handling comprehensive image generation tasks, as exemplified by models like ACE [18] and OmniGen [54]. Research on unified image generation foundation models is garnering increasing attention as it reduces the semantic gap between the pre-trained models and

practical applications, and significantly lowers the costs associated with task-specific customization.

Despite this growing research trend, the development of automatic evaluation benchmarks for unified image generation remains significantly lagging. Early evaluation frameworks primarily relied on datasets such as CUB-200-2011 [38, 50], Oxford Flower-102[31], and MS-COCO [26], and utilized Fréchet Inception Distance (FID) [20] and Inception Score (IS) [42] as metrics to quantify the performance. However, these data and metrics are primarily tailored for text-to-image creating, limiting their ability to assess global description-guided generation, could not reflect the comprehensive capability of a unified image generation model. Recently some image editing benchmarks [5, 44, 57] have been proposed to assess model performance on general-purpose instruction-based image editing tasks. While these benchmarks provide valuable insights, they exhibit several limitations when used to evaluate unified image generation models: (1) *Limited Evaluation Scope*. As illustrated in Tab. 1, existing datasets are typically tailored for one or a few specific tasks, resulting in evaluation outcomes that are biased toward these particular tasks. (2) *Insufficient Evaluation Granularity and Dimensions*: Current evaluation frameworks predominantly rely on metrics such as FID and IS for assessing image quality, and CLIP [36] similarity for image-condition consistency. However, these metrics are inadequate for comprehensive evaluation and often misalign with human preferences. As a result, human evaluation is often necessary, making the process both time-consuming and costly. (3) *Bias in Data Distribution*: Most existing benchmarks suffer from data bias issues. For example, InstructPix2Pix [5] includes only synthesized images, while MagicBrush [57] contains only real images. This limitation hampers the ability to evaluate model performance across diverse data sources.

Given these limitations, there is an urgent need for a unified and comprehensive benchmark to evaluate image generation models both automatically and effectively. Therefore, we propose **ICE-Bench**, an extensive benchmark designed for the holistic evaluation of unified image generation. As demonstrated in Tab. 1, the strengths of our ICE-Bench can be encapsulated in three key aspects: *coarse-to-fine tasks*, *multi-dimensional metrics*, and *hybrid data*.

First, we establish a **hierarchical evaluation task set** that decomposes image generation capabilities into coarse-to-fine granularity. As shown in Fig. 1, the evaluation tasks are categorized into 2 dimensions at a coarse-grained dimensions based on generation type (creating and editing). Each of them is further divided into 2 medium-grained categories based on dependency on a reference (Ref or Non-Ref). Then 31 specific tasks are broken down into more refined categories, considering controllable generation, global editing, local editing, style transferring, etc. Based on these

Table 1. Comparison with existing image generation datasets.

| Datasets | Publications | Creating | Editing | Training | Evaluation | #Evaluation Data | #Evaluation Tasks |
|---------------------------|------------------------------------|----------|---------|----------|----------------|------------------|-------------------|
| CUB-200-2011 [38, 50] | Caltech techreport 2011, CVPR 2016 | ✓ | | ✓ | ✓ | 2,933 | 1 |
| Oxford Flower-102 [31] | ICVGIP 2008 | ✓ | | ✓ | ✓ | 2,040 | 1 |
| MS-COCO [26] | ECCV 2014 | ✓ | | ✓ | ✓ | 40,000 | 1 |
| DrawBench [41] | NeurIPS 2022 | ✓ | | | ✓ (Human-eval) | 200 | 1 |
| Multi-Task Benchmark [34] | NeurIPS 2022 | ✓ | | | ✓ (Human-eval) | 3,600 | 1 |
| PAINTSKILLS [12] | ICCV 2023 | ✓ | | | ✓ | 7,185 | 1 |
| EditBench [52] | CVPR 2023 | | ✓ | | ✓ | 240 | 1 |
| InstructPix2Pix [5] | CVPR 2023 | | ✓ | ✓ | | - | 4 |
| MagicBrush [57] | NeurIPS 2023 | | ✓ | ✓ | ✓ | 1,053 | 5 |
| UltraEdit [60] | NeurIPS 2024 | | ✓ | ✓ | | - | 9+ |
| HIVE [59] | CVPR 2024 | | ✓ | ✓ | ✓ | 1,000 | 1 |
| Emu Edit [44] | CVPR 2024 | | ✓ | | ✓ | 3,055 | 7 |
| ICE-Bench | This paper | ✓ | ✓ | | ✓ | 6,538 | 31 |

31 coarse-to-fine evaluation tasks, the model’s generation ability can be comprehensively evaluated.

Second, in conjunction with the evaluation tasks, we have planned **6 evaluation dimensions** to effectively evaluate the model capabilities, including aesthetic quality, imaging quality, prompt following, source consistency, reference consistency, and controllability. These dimensions are quantified using 11 specialized metrics, providing targeted insights into model performance and guiding improvements in model architecture, training data, and strategies.

Third, we curate a **hybrid dataset** that includes both real-world and virtually generated images. In this way, data diversity is effectively promoted, and the bias problem in evaluation is alleviated.

We conduct extensive experiments and evaluate the generation capability of 10 state-of-the-art generation models, including both general-purpose and task-specific models. The experimental results highlight their strengths and weaknesses across various tasks and dimensions. We are open-sourcing ICE-Bench, including data, evaluation script, and models, to encourage broader participation in advancing image generation research and fostering fair, comprehensive, and unified evaluation practices.

2. Related work

2.1. Text-to-image Creating Benchmark

In the early stages, CUB-200-2011 [38, 50], Oxford Flower-102 [31], and MS-COCO [26] were commonly used to evaluate generation capabilities. These datasets primarily focus on a single generation task, namely text-to-image creating, and are domain-specific. For instance, CUB-200-2011 and Oxford Flower-102 are limited to specific categories such as birds and flowers, respectively. This narrow focus makes it challenging to assess the performance of generation models in real-world applications. Moreover, these datasets primarily evaluate two aspects: image quality and instruc-

tion alignment, using metrics such as FID [20] and CLIP score [36]. To further evaluate the generation models’ visual reasoning skills, PAINTSKILLS [12] was proposed, which could measure three fundamental visual reasoning abilities, i.e., object recognition, object counting, and spatial relation understanding. To assess text-to-image models in greater depth, DrawBench [41] was proposed to assess capabilities such as rendering colors, object counts, spatial relationships, and text within scenes. However, DrawBench relies on human evaluation, which limits its generalizability, a limitation shared by the Multi-Task Benchmark [34].

2.2. Image Editing Benchmark

While the aforementioned datasets are primarily designed for text-to-image creating task, image editing has become a fundamental practice in today’s digital landscape, playing a crucial role in fields such as photography, advertising, and social media. Consequently, researchers have begun to develop datasets specifically for image editing tasks. InstructPix2Pix [5] and UltraEdit [60] leverage LLMs such as GPT-3 [6] and GPT-4 [1], to generate the image editing instructions. It is noted that these datasets are primarily used for training generation models rather than evaluation. Similarly, HIVE [59], although containing evaluation data, is designed for training purposes, utilizing human feedback for instructional image editing. And it also focuses on a single editing task: generating an image based on an original image and an instruction. MagicBrush [57] and Emu Edit [44] cover multiple editing tasks, i.e., 5 and 7 types, respectively. However, these datasets still fall short of providing a comprehensive evaluation of generative models’ capabilities.

Given the limitations of existing datasets, it remains challenging to evaluate the capabilities of generation models comprehensively. To this end, we propose **ICE-Bench**, a benchmark that includes 31 fine-grained creating and editing tasks, and 11 evaluation metrics taking account of aesthetic quality, imaging quality, prompt following, source

consistency, reference consistency, and controllability.

3. ICE-Bench

In this section, we introduce ICE-Bench, our proposed benchmark for evaluating image generation models. We first elaborate on the overall 31 image generation tasks in Sec. 3.1, which are categorized into 4 groups, in terms of the format of input data. Next, we detail the evaluation metrics in Sec. 3.2, which are designed to comprehensively assess the generation capabilities of existing models across 6 dimensions. Finally, in Sec. 3.3, we introduce the overall data construction pipeline to show its reliability.

3.1. Evaluation Tasks

Recall that ICE-Bench aims to comprehensively evaluate the model capability in the multi-modal guided image generation field. To achieve this goal, we first curate and design 31 specific image generation tasks. Examples of these tasks are illustrated in Fig. 1 of Supplementary File. Despite the diverse final objectives of these tasks, we find that only up to three types of inputs are necessary for all existing image generation tasks: (1) *Textual prompt*, could be the user’s instructions or descriptions for the generated image. (2) *Source image*, provides to accommodate specific regional editing requests while maintaining pixel consistency in areas unrelated to the editing requests. (3) *Reference images*, provides reference on some aspects, typically specified by the instruction.

Based on the presence or absence of a source image and reference images, 31 tasks are classified into 4 categories: (1) *No-ref Image Creating*, which relies solely on a textual prompt as the condition; (2) *No-ref Image Editing*, which requires both a textual prompt and a source image as input; (3) *Ref Image Creating*, which necessitates a textual prompt along with reference images; and (4) *Ref Image Editing*, which demands all three types of inputs for generation.

3.1.1. No-ref Image Creating

- **Task 1: Text-to-Image Creating.** Generate an image based solely on a given textual prompt.

3.1.2. Ref Image Creating

- **Tasks 2-4: Face/Style/Subject Reference Creating.** These tasks require generating an image that adheres to a textual prompt while maintaining consistency with a reference image in terms of *facial features, style, or subject*.

3.1.3. No-ref Image Editing

Here we further split the generation capabilities in disentangled 3 aspects: *global editing, local editing, and controllable generation*.

Global Editing:

- **Tasks 5-8: Color/Motion/Face/Texture Editing.** These tasks involve modifying specific *attributes* (e.g., *color,*

motion, facial features, or texture) of a source image based on textual instructions.

- **Task 9: Style Editing.** Change the style of a source image to match a specified style described in the instruction.
- **Task 10: Scene Editing.** Following the instruction, alter the background of the source image, to a specific scene.
- **Tasks 11-13: Subject Addition/Removal/Change.** According to the instructions, *add, delete or change an object to another object* on the given source image, while preserving other regions.
- **Tasks 14-15: Text Render/Removal.** Render some text in source image at location specified by instruction or remove all text.
- **Task 16: Composite Editing.** Perform multiple edits on a source image based on instructions.

Local Editing:

- **Task 17: Inpainting.** Repaint a specific region of the source image, identified by a mask image, with content specified by a textual description or instructions.
- **Task 18: Outpainting.** Expand the source image beyond its original boundary based on a mask and textual prompt.
- **Tasks 19-20: Local Subject Addition/Removal.** Like subject addition/removal, but the location is indicated by a mask.
- **Tasks 21-22: Local Text Render/Removal.** Like text render/removal, but the location is indicated by a mask.

Controllable Generation:

- **Tasks 23-25: Pose/Edge/Depth-guided Generation.** Generate an image that aligns with the given *pose/edge/depth* map.
- **Task 26: Image Colorization.** Given a gray image as source image, colorize it by following the textual prompt.
- **Task 27: Image Deblurring.** Given a low-quality or blurred image, make it clear and improve its quality.

3.1.4. Ref Image Editing

- **Task 28: Style Transfer.** Transfer the style of a reference image to a source image.
- **Task 29: Subject-guided Inpainting.** Incorporate a subject from a reference image into a specific region of a source image, as indicated by a mask image.
- **Task 30: Virtual Try On.** A specialized application of subject-guided inpainting focused on rendering clothing items realistically on human subjects.
- **Task 31: Face Swap.** Regenerate the face in the masked area of the source image by referencing the facial features of the reference image.

3.2. Evaluation Metrics

We assess the performance of existing generative models across 6 dimensions: *aesthetic quality, imaging qual-*

ity, prompt following, source consistency, reference consistency, and controllability, as illustrated in Fig. 1. Here we present the metrics employed for each evaluation dimension. Detailed calculation equations can be found in the Supplementary Material.

3.2.1. Aesthetic Quality

We assess the *aesthetic score* of generated images using the Aesthetic Predictor¹, which reflects the overall aesthetic appeal of the generated image, considering multiple aspects such as layout, colorfulness, harmony, naturalness, and photo-realism.

3.2.2. Imaging Quality

The imaging quality assessment focuses mainly on aspects such as blur, noise, distortion, and overexposure. We utilize the MUSIQ [23] quality predictor as the *imaging score*. To ensure a fair comparison, we resize all generated images to same shape, which tends to favor high-resolution images.

3.2.3. Prompt Following

For image creating tasks, we measure prompt following using the *CLIP similarity* between the text prompt and the generated image. While, for image editing tasks, we dissect the prompt following ability into two aspects, i.e., visual-language alignment, and instruction execution reasoning. It is noted that we make the best use of the powerful ability of VLLM in these two evaluations. Firstly, for each test case, a reasonable description of target image is inferred by providing a VLLM with all input conditions. Then we calculate the CLIP similarity between the generated image and the given caption to reflect the degree of prompt following, denoted as *CLIP-cap*. Secondly, we newly introduce a *VLLM-QA* metric to assess whether an edit instruction has been successfully executed, utilizing the reasoning ability of VLLM. Given the textual instruction, source image, reference images, and the generated image, we prompt VLLM, i.e., Qwen2-VL-72B [51], to determine the success of the generation. A successful generation returns a value of 1, otherwise returns 0.

3.2.4. Source Consistency

For image editing tasks, we evaluate the semantic consistency and pixel alignment between the source image and the generated image, based on the principle that any image editing request needs retain some pixel unchanged to some extent. We calculate CLIP similarity for semantic consistency and mean L1 distance for pixel alignment between source image and generated image, denoted as *CLIP-src* and *L1-src*, respectively.

3.2.5. Reference Consistency

For reference-based tasks, the reference consistency should be considered from different dimensions in terms of the task

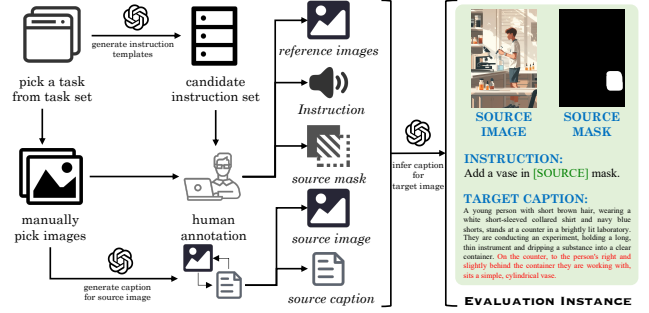


Figure 2. The overall pipeline of dataset construction.

objective. In our ICE-Bench, we mainly focus on three types of reference: face, subject and style. For face reference, we calculate the *face similarity* using the buffalo model from InsightFace App [14]. For subject reference, we calculate the *DINO* [9] similarity between the reference image and generated image. For style reference, we use the CSD [45] model to extract feature as style descriptor, then calculate the similarity between reference image and generated image, denoted as *Style-ref*.

3.2.6. Controllability

Controllable generation aims to generate an artistic image under the control of some low-level visual cues, such as edge map, depth map, pose map, etc. We use diverse metrics that tailored for difference control conditions to comprehensively evaluate the controllability of models: (1) For pose, depth and edge-guided generation tasks, we extract the low-level feature of generated image [7, 8, 37] and then calculate the mean l1 distance between the input and the extracted feature maps. (2) For image colorization task, we calculate the colorfulness score [19] of generated image, and then calculate the mean l1 distance between the input image and the grayscale generated image. (3) For image deblurring task, we calculate the SSIM [53] score between the source image and generated image.

3.3. Dataset Construction

Collecting a dataset for 31 fine-grained evaluation tasks demands a significant investment of both human resources and time. To streamline this process, we have designed a data construction pipeline that integrates large pre-trained models with human annotation, as depicted in Fig. 2. The pipeline begins with the manual selection of source and reference images from hybrid datasets such as MSCOCO [26], LAION-5B [43], DreamBooth [40], VITON-HD [13] and synthetic image databases. Next, we utilize VLLMs to generate descriptions for the chosen source images and provide task-specific instruction templates. Based on the instruction templates, we request annotators to craft unique instructions for each case, taking into account the selected source image and reference image. The annotation

¹<https://github.com/discus0434/aesthetic-predictor-v2-5>

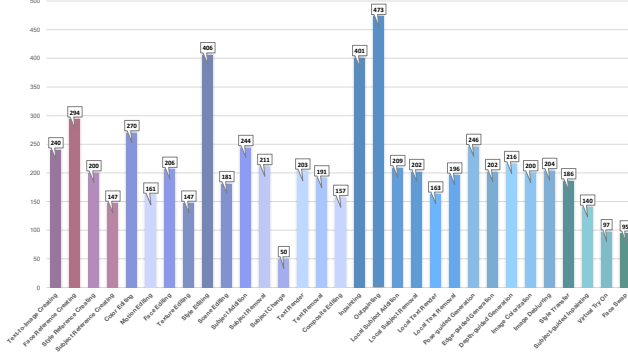


Figure 3. Data distribution of each task in ICE-Bench .

process follows rigorous standards to ensure the accuracy and reliability. Finally, using all the available data, we ask VLLM to envision the content of an ideal generated image and to produce a detailed description of this imagined image. In total, we collect 6,538 instances across all tasks. The distribution of the dataset is detailed in Fig. 3.

4. Experiments

4.1. Evaluation Models

We select 10 mainstream image generation models to comprehensively evaluate their capabilities in 31 tasks from 6 diverse aspects, which have been introduced in Sec. 3, including OmniGen [54], OminiControl [47], ACE [18], ACE++ [29], FLUX [25], FLUX-Control [48], InstructPix2Pix [5], MagicBrush [57], UltraEdit [60], IP-Adapter [56]. All evaluation metrics are designed such that higher values indicate better performance.

However, it is important to note that not all models are designed to excel in every evaluation task. For example, FLUX is limited to text-to-image creating, while OminiControl specialize in subject reference creating and controllable generation tasks. To ensure a fair comparison, we first evaluate each model on its designated tasks and subsequently conduct a comprehensive cross-task analysis. For tasks that a model cannot address, its score is set to zero. Detailed task-perspective and model-perspective analysis are presented in Sec. 4.3 and Sec. 4.4, respectively.

4.2. Evaluation Setting

All experiments are conducted using the Diffusers² framework for model implementation. For models not yet integrated into Diffusers, we utilize their official implementations. All generation and evaluation processes are performed on A100 GPU cards, with default hyper-parameters for each model to ensure consistency and reproducibility.

²<https://github.com/huggingface/diffusers>

Table 2. Model performance on No-ref Image Creating Task (Task 1).

| Models | AES↑ | IMG↑ | PF↑ |
|---------|--------------|--------------|--------------|
| ACE | 0.548 | 0.534 | 0.566 |
| OmniGen | 0.611 | 0.726 | 0.570 |
| FLUX | 0.618 | 0.735 | 0.570 |

4.3. Task-perspective Evaluation and Comparison

Given the extensive scope of evaluation tasks, we categorize the comparison into four task settings: *No-ref Image Creating*, *Ref Image Creating*, *No-ref Image Editing*, *Ref Image Editing*, as introduced in Sec. 3.1. Here, we present the evaluation results for these four task subgroups, with the specific score values for each task detailed in the Supplementary Material.

4.3.1. Evaluation on No-ref Image Creating Tasks

There is only one task belonging to this group, *i.e.*, text-to-image creating, and 3 models, *i.e.*, ACE, OmniGen, and FLUX, favor this task. We assess their performance from 3 aspects including aesthetic quality (AES), imaging quality (IMG) and prompt following (PF), as shown in Tab. 2.

4.3.2. Evaluation on Ref Image Creating Tasks

We evaluate models on face, style, and subject reference creating tasks, to assess their ability for extracting and applying key features from reference images. Performance is measured using four metrics: aesthetic quality (AES), imaging quality (IMG), prompt following (PF) and reference consistency (REF). The results are reported in Tab. 3.

4.3.3. Evaluation on No-ref Image Editing Tasks

Considering the type of source image and the necessity for a source image mask, we further categorize the No-Reference Image Editing tasks into three subgroups: Controllable Generation, Global Editing, and Local Editing. For each subgroup, we compute average scores across evaluation dimensions to determine overall performance. Aesthetic quality (AES), imaging quality (IMG), and prompt following (PF) are evaluated in all three subgroup. Besides, controllability (CTRL) is assessed in controllable Generation, and source consistency (SRC) is assessed in both global and local editing. The experimental results are presented in Tab. 4.

4.3.4. Evaluation on Ref Image Editing Tasks

Like Ref Image Creating tasks, we evaluate the reference consistency using face, style and subject. Notably, we evaluate on virtual try on and subject-guided inpainting tasks for subject reference editing, and average their scores for final performance. Besides, source consistency (SRC) is assessed. The results are provided in Tab. 5.

Table 3. Model performance on Ref Image Creating Tasks.

| Models | Face Reference (Task 2) | | | | Style Reference (Task 3) | | | | Subject Reference (Task 4) | | | |
|--------------|-------------------------|--------------|--------------|--------------|--------------------------|--------------|--------------|--------------|----------------------------|--------------|--------------|--------------|
| | AES↑ | IMG↑ | PF↑ | REF↑ | AES↑ | IMG↑ | PF↑ | REF↑ | AES↑ | IMG↑ | PF↑ | REF↑ |
| ACE | 0.535 | 0.550 | 0.531 | 0.329 | 0.531 | 0.590 | 0.232 | 0.802 | 0.523 | 0.557 | 0.498 | 0.878 |
| OmniGen | 0.579 | 0.727 | 0.541 | 0.573 | 0.579 | 0.708 | 0.431 | 0.432 | 0.582 | 0.714 | 0.532 | 0.753 |
| IP-Adapter | 0.505 | 0.642 | 0.508 | 0.633 | 0.577 | 0.696 | 0.288 | 0.749 | 0.573 | 0.703 | 0.484 | 0.841 |
| ACE++ | 0.551 | 0.679 | 0.523 | 0.506 | - | - | - | - | 0.520 | 0.628 | 0.475 | 0.853 |
| OminiControl | - | - | - | - | - | - | - | - | 0.565 | 0.723 | 0.528 | 0.783 |

Table 4. Model performance on No-Ref Image Editing Tasks. It should be noted that OminiControl lacks pose-guided generation capability, which results in its average score in Controllable Generation being significantly lower than that of other methods.

| Models | Global Editing (Tasks 5-16) | | | | Local Editing (Tasks 17-22) | | | | Controllable Generation (Tasks 23-27) | | | |
|-----------------|-----------------------------|--------------|--------------|--------------|-----------------------------|--------------|--------------|--------------|---------------------------------------|--------------|--------------|--------------|
| | AES↑ | IMG↑ | PF↑ | SRC↑ | AES↑ | IMG↑ | PF↑ | SRC↑ | AES↑ | IMG↑ | PF↑ | CTRL↑ |
| ACE | 0.498 | 0.521 | 0.567 | 0.899 | 0.492 | 0.490 | 0.615 | 0.919 | 0.545 | 0.505 | 0.630 | 0.865 |
| OmniGen | 0.490 | 0.598 | 0.520 | 0.844 | 0.464 | 0.562 | 0.503 | 0.853 | 0.510 | 0.594 | 0.592 | 0.783 |
| InstructPix2Pix | 0.480 | 0.518 | 0.355 | 0.758 | - | - | - | - | - | - | - | - |
| MagicBrush | 0.456 | 0.486 | 0.444 | 0.840 | - | - | - | - | - | - | - | - |
| UltraEdit | 0.490 | 0.504 | 0.470 | 0.866 | 0.454 | 0.455 | 0.432 | 0.953 | - | - | - | - |
| FLUX-Control | - | - | - | - | - | - | - | - | 0.552 | 0.534 | 0.609 | 0.846 |
| ACE++ | - | - | - | - | 0.495 | 0.588 | 0.606 | 0.933 | - | - | - | - |
| OminiControl* | - | - | - | - | - | - | - | - | 0.416 | 0.380 | 0.451 | 0.687 |

Table 5. Model performance on Ref Image Editing Tasks.

| Models | Style Transfer (Task 28) | | | | | Subject Reference (Tasks 29-30) | | | | | Face Swap (Task 31) | | | | |
|---------|--------------------------|--------------|--------------|--------------|--------------|---------------------------------|--------------|--------------|--------------|--------------|---------------------|--------------|--------------|--------------|--------------|
| | AES↑ | IMG↑ | PF↑ | REF↑ | SRC↑ | AES↑ | IMG↑ | PF↑ | REF↑ | SRC↑ | AES↑ | IMG↑ | PF↑ | REF↑ | SRC↑ |
| ACE | 0.535 | 0.530 | 0.350 | 0.234 | 0.788 | 0.483 | 0.586 | 0.415 | 0.657 | 0.909 | 0.498 | 0.570 | 0.432 | 0.250 | 0.873 |
| OmniGen | 0.505 | 0.630 | 0.338 | 0.359 | 0.701 | 0.458 | 0.667 | 0.414 | 0.650 | 0.821 | 0.431 | 0.640 | 0.459 | 0.477 | 0.775 |
| ACE++ | - | - | - | - | - | 0.471 | 0.685 | 0.480 | 0.663 | 0.892 | 0.503 | 0.650 | 0.452 | 0.378 | 0.853 |

4.4. Model-perspective Evaluation and Comparison

We present a comprehensive evaluation of the models across all 31 tasks. The final score for each task is computed as a weighted sum of scores from multiple evaluation dimensions. Tasks unsupported by a model are assigned a score of zero. The results are visualized in Fig. 4.

4.5. Qualitative Analysis of Metric Effectiveness

In Fig. 5, we qualitatively evaluate the effectiveness of our benchmark through three representative cases. In the first case, all models generate images containing a burger, fries, a plate, and orange juice, aligning with the instruction. This aligns with the PF scores in Tab. 2, where all models achieve comparable results. However, OmniGen and FLUX generate images with superior aesthetic quality and imaging quality, consistent with quantitative evaluations. In the style referenced creating, ACE exhibits a “copy-paste” issue, achieving high reference consistency but failing to adhere to the prompt. IP-Adapter strikes a better balance between prompt adherence and reference consistency. For local editing, ACE++ outperforms other models, demonstrating precise prompt adherence and high aesthetic quality. In contrast, OmniGen fails to interpret the editing instruction, returning a masked image, which highlights its inadequate training for pixel-aligned editing tasks. These

qualitative observations validate the robustness and discriminative power of our metrics.

5. Insights and Discussions

In this section, we present the key observations and insights derived from our comprehensive evaluation experiments.

(1) Limited generality of existing image generation models. From Fig. 4, it is evident that most existing image generation methods are task-specific, with limited generality. Although ACE and OmniGen support all evaluated tasks, their performance remains unsatisfactory in certain areas. Both models achieve low reference consistency scores on the Style Transfer task (0.234 for ACE and 0.359 for OmniGen) and perform poorly on the Face Swap task in terms of reference consistency and aesthetic quality. These limitations underscore the need for developing more versatile and general-purpose generation models capable of handling diverse tasks effectively, and also highlights the importance of conducting unified and comprehensive evaluations, which is exactly what ICE-Bench aims to achieve.

(2) Training data quality and model scalability significantly impact imaging quality. Our experiments demonstrate a strong correlation between model scalability, training data quality, and imaging performance. In general, larger models trained with high-resolution images consis-

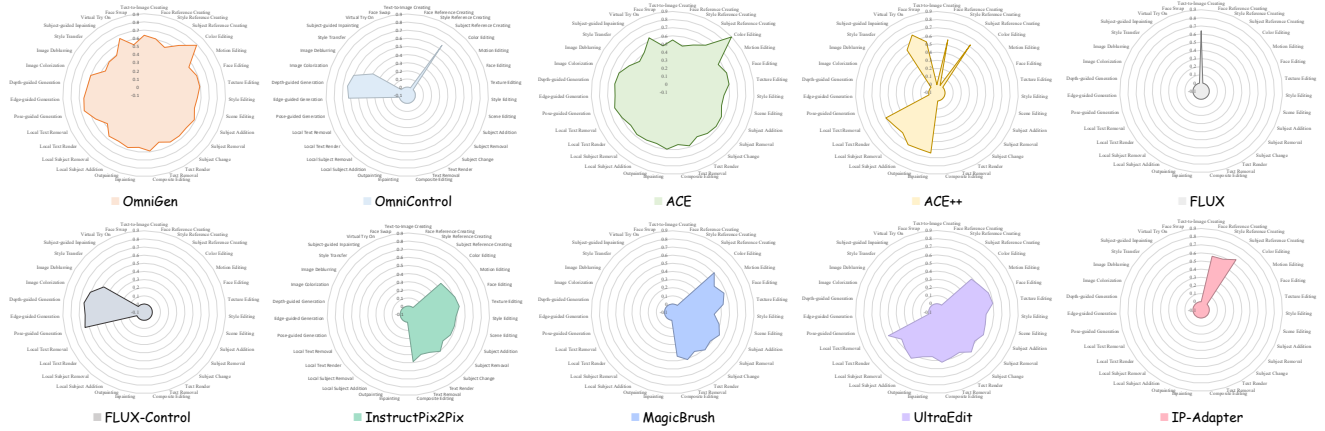


Figure 4. Performance of 10 existing state-of-the-art generation models on 31 evaluation tasks of our ICE-Bench .

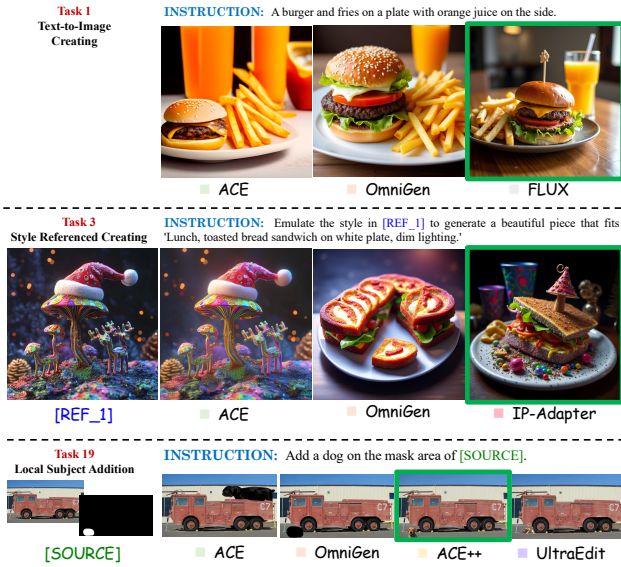


Figure 5. Examples of generation results on 3 tasks.

tently exhibit superior image generation capabilities. For instance, as shown in Tab. 2 and Tab. 3, OmniGen, with 3.8 billion parameters and trained on images up to 2280×2280 resolution, significantly outperforms ACE, which is limited to 0.6 billion parameters and a maximum resolution of 512×512 . This disparity underscores the critical role of model capacity and high-quality training data in achieving high-fidelity image generation. These findings suggest that future research should prioritize scaling model architectures and improving data quality over merely increasing data size.

(3) Trade-off across evaluation dimensions. As evidenced in Tab. 3, a notable trade-off exists between reference consistency and prompt adherence. Models that excel in reference consistency, often underperform in prompt adherence. For instance, ACE achieves high reference consistency scores (0.849 for style reference and 0.864 for subject reference) but struggles with prompt adherence, indicating

a tendency toward “copy-paste” behavior. This highlights the inherent challenge in balancing precise prompt following with maintaining contextual and stylistic consistency, a critical area for future model improvements.

(4) Effectiveness of pixel-aligned image editing data. Regarding SRC, Tab. 4 and Tab. 5 reveal that OmniGen performs significantly worse compared to other models. We attribute this to OmniGen’s inadequate training for pixel-aligned image editing tasks. In contrast, ACE, UltraEdit, and ACE++ allocate a higher proportion of training samples to pixel-aligned editing, which enhances their source consistency capabilities. Notably, although InstructPix2Pix and MagicBrush are designed for pixel-aligned editing, their performance is hindered by limited and low-quality training data, resulting in subpar performance across all metrics.

6. Conclusion and Future Work

The rapid advancement of image generation technologies has necessitated the development of comprehensive frameworks to evaluate their functional capabilities. In this paper, we propose a *unified and comprehensive benchmark, termed ICE-Bench*, to evaluate the generation capabilities of existing models. ICE-Bench incorporates 31 *fine-grained generation tasks* organized in a coarse-to-fine hierarchy, 6 *evaluation dimensions supported by 11 metrics*, and 6,538 *task instances* encompassing both real-world and synthetically generated images. This benchmark enables a thorough evaluation of model performance across multiple dimensions, including *aesthetic quality*, *imaging quality*, *prompt following*, *source consistency*, *reference consistency*, and *controllability*, thereby fostering innovation and breakthroughs in the field of image generation.

Building on ICE-Bench, we are developing a *leaderboard*, a quantifiable and comparative framework that benchmarks the capabilities of existing models, thereby fostering transparency, competition, and continuous advancement in image generation.

References

- [1] Josh Achiam, Steven Adler, Sandhini Agarwal, Lama Ahmad, Ilge Akkaya, Florencia Leoni Aleman, Diogo Almeida, Janko Altenschmidt, Sam Altman, Shyamal Anadkat, et al. Gpt-4 technical report. *arXiv preprint arXiv:2303.08774*, 2023. 3
- [2] Runway AI. Stable Diffusion v1.5 Model Card, <https://huggingface.co/runwayml/stable-diffusion-v1-5>, 2022. 2
- [3] Runway AI. Stable Diffusion Inpainting Model Card, <https://huggingface.co/runwayml/stable-diffusion-inpainting>, 2022. 2
- [4] James Betker, Gabriel Goh, Li Jing, Tim Brooks, Jianfeng Wang, Linjie Li, Long Ouyang, Juntang Zhuang, Joyce Lee, Yufei Guo, et al. Improving image generation with better captions. *Computer Science*. <https://cdn.openai.com/papers/dall-e-3.pdf>, 2(3):8, 2023. 2
- [5] Tim Brooks, Aleksander Holynski, and Alexei A Efros. Instructpix2pix: Learning to follow image editing instructions. In *Proceedings of the IEEE/CVF Conference on Computer Vision and Pattern Recognition*, pages 18392–18402, 2023. 2, 3, 6, 13
- [6] Tom Brown, Benjamin Mann, Nick Ryder, Melanie Subbiah, Jared D Kaplan, Prafulla Dhariwal, Arvind Neelakantan, Pranav Shyam, Girish Sastry, Amanda Askell, et al. Language models are few-shot learners. *Advances in neural information processing systems*, 33:1877–1901, 2020. 3
- [7] John Canny. A Computational Approach to Edge Detection. *IEEE TPAMI*, pages 679–698, 1986. 5
- [8] Zhe Cao, Gines Hidalgo, Tomas Simon, Shih-En Wei, and Yaser Sheikh. OpenPose: Realtime Multi-Person 2D Pose Estimation Using Part Affinity Fields. *IEEE TPAMI*, 43(1): 172–186, 2021. 5
- [9] Mathilde Caron, Hugo Touvron, Ishan Misra, Hervé Jégou, Julien Mairal, Piotr Bojanowski, and Armand Joulin. Emerging properties in self-supervised vision transformers. In *Proceedings of the IEEE/CVF international conference on computer vision*, pages 9650–9660, 2021. 5
- [10] Chaofeng Chen and Jiadi Mo. IQA-PyTorch: Pytorch toolbox for image quality assessment. [Online]. Available: <https://github.com/chaofengc/IQA-PyTorch>, 2022. 12
- [11] Xi Chen, Lianghua Huang, Yu Liu, Yujun Shen, Deli Zhao, and Hengshuang Zhao. AnyDoor: Zero-shot Object-level Image Customization. *arXiv preprint arXiv:2307.09481*, 2023. 2
- [12] Jaemin Cho, Abhay Zala, and Mohit Bansal. Dall-eval: Probing the reasoning skills and social biases of text-to-image generation models. In *Proceedings of the IEEE/CVF International Conference on Computer Vision*, pages 3043–3054, 2023. 3
- [13] Seunghwan Choi, Sunghyun Park, Minsoo Lee, and Jaegul Choo. VITON-HD: High-Resolution Virtual Try-On via Misalignment-Aware Normalization. In *CVPR*, pages 14131–14140, 2021. 5
- [14] deepinsight. insightface. <https://github.com/deepinsight/insightface>, 2021. 5
- [15] Patrick Esser, Sumith Kulal, Andreas Blattmann, Rahim Entezari, Jonas Müller, Harry Saini, Yam Levi, Dominik Lorenz, Axel Sauer, Frederic Boesel, Dustin Podell, Tim Dockhorn, Zion English, Kyle Lacey, Alex Goodwin, Yannik Marek, and Robin Rombach. Scaling Rectified Flow Transformers for High-Resolution Image Synthesis. In *ICML*, 2024. 2
- [16] Ian Goodfellow, Jean Pouget-Abadie, Mehdi Mirza, Bing Xu, David Warde-Farley, Sherjil Ozair, Aaron Courville, and Yoshua Bengio. Generative adversarial nets. *Advances in neural information processing systems*, 27, 2014. 2
- [17] Jian Han, Jinlai Liu, Yi Jiang, Bin Yan, Yuqi Zhang, Zehuan Yuan, Bingyue Peng, and Xiaobing Liu. Infinity: Scaling bit-wise autoregressive modeling for high-resolution image synthesis. *arXiv preprint arXiv:2412.04431*, 2024. 2
- [18] Zhen Han, Zeyinzi Jiang, Yulin Pan, Jingfeng Zhang, Chaojie Mao, Chenwei Xie, Yu Liu, and Jingren Zhou. Ace: All-round creator and editor following instructions via diffusion transformer. *arXiv preprint arXiv:2410.00086*, 2024. 2, 6, 13
- [19] David Hasler and Sabine E Suesstrunk. Measuring colorfulness in natural images. In *Human vision and electronic imaging VIII*, pages 87–95. SPIE, 2003. 5
- [20] Martin Heusel, Hubert Ramsauer, Thomas Unterthiner, Bernhard Nessler, and Sepp Hochreiter. Gans trained by a two time-scale update rule converge to a local nash equilibrium. *Advances in neural information processing systems*, 30, 2017. 2, 3
- [21] Jonathan Ho, Ajay Jain, and Pieter Abbeel. Denoising diffusion probabilistic models. *Advances in neural information processing systems*, 33:6840–6851, 2020. 2
- [22] Zeyinzi Jiang, Chaojie Mao, Yulin Pan, Zhen Han, and Jingfeng Zhang. SCEdit: Efficient and Controllable Image Diffusion Generation via Skip Connection Editing. In *CVPR*, pages 8995–9004, 2024. 2
- [23] Junjie Ke, Qifei Wang, Yilin Wang, Peyman Milanfar, and Feng Yang. Musiq: Multi-scale image quality transformer. In *Proceedings of the IEEE/CVF international conference on computer vision*, pages 5148–5157, 2021. 5
- [24] Diederik P Kingma and Max Welling. Auto-encoding variational bayes. *arXiv preprint arXiv:1312.6114*, 2013. 2
- [25] Black Forest Labs. Flux. <https://github.com/black-forest-labs/flux>, 2024. 2, 6, 13
- [26] Tsung-Yi Lin, Michael Maire, Serge Belongie, James Hays, Pietro Perona, Deva Ramanan, Piotr Dollár, and C Lawrence Zitnick. Microsoft coco: Common objects in context. In *Computer Vision—ECCV 2014: 13th European Conference, Zurich, Switzerland, September 6–12, 2014, Proceedings, Part V 13*, pages 740–755. Springer, 2014. 2, 3, 5
- [27] Xingchao Liu, Chengyue Gong, and Qiang Liu. Flow straight and fast: Learning to generate and transfer data with rectified flow. *arXiv preprint arXiv:2209.03003*, 2022. 2
- [28] Simian Luo, Yiqin Tan, Longbo Huang, Jian Li, and Hang Zhao. Latent consistency models: Synthesizing high-resolution images with few-step inference. *arXiv preprint arXiv:2310.04378*, 2023. 2

- [29] Chaojie Mao, Jingfeng Zhang, Yulin Pan, Zeyinzi Jiang, Zhen Han, Yu Liu, and Jingren Zhou. Ace++: Instruction-based image creation and editing via context-aware content filling. *arXiv preprint arXiv:2501.02487*, 2025. 6, 13
- [30] Chenlin Meng, Yutong He, Yang Song, Jiaming Song, Jiajun Wu, Jun-Yan Zhu, and Stefano Ermon. Sdedit: Guided image synthesis and editing with stochastic differential equations. *arXiv preprint arXiv:2108.01073*, 2021. 2
- [31] Maria-Elena Nilsback and Andrew Zisserman. Automated flower classification over a large number of classes. In *2008 Sixth Indian conference on computer vision, graphics & image processing*, pages 722–729. IEEE, 2008. 2, 3
- [32] Yulin Pan, Chaojie Mao, Zeyinzi Jiang, Zhen Han, Jingfeng Zhang, and Xiangteng He. Locate, assign, refine: Taming customized promptable image inpainting. *arXiv preprint arXiv:2403.19534*, 2024. 2
- [33] William Peebles and Saining Xie. Scalable diffusion models with transformers. In *Proceedings of the IEEE/CVF international conference on computer vision*, pages 4195–4205, 2023. 2
- [34] Vitali Petsiuk, Alexander E Siemenn, Saisamrit Surbehera, Zad Chin, Keith Tyser, Gregory Hunter, Arvind Raghavan, Yann Hicke, Bryan A Plummer, Ori Kerret, et al. Human evaluation of text-to-image models on a multi-task benchmark. *arXiv preprint arXiv:2211.12112*, 2022. 3
- [35] Dustin Podell, Zion English, Kyle Lacey, Andreas Blattmann, Tim Dockhorn, Jonas Müller, Joe Penna, and Robin Rombach. Sdxl: Improving latent diffusion models for high-resolution image synthesis. *arXiv preprint arXiv:2307.01952*, 2023. 2
- [36] Alec Radford, Jong Wook Kim, Chris Hallacy, Aditya Ramesh, Gabriel Goh, Sandhini Agarwal, Girish Sastry, Amanda Askell, Pamela Mishkin, Jack Clark, et al. Learning transferable visual models from natural language supervision. In *International conference on machine learning*, pages 8748–8763. PmlR, 2021. 2, 3, 13
- [37] René Ranftl, Katrin Lasinger, David Hafner, Konrad Schindler, and Vladlen Koltun. Towards Robust Monocular Depth Estimation: Mixing Datasets for Zero-Shot Cross-Dataset Transfer. *IEEE TPAMI*, pages 1623–1637, 2022. 5
- [38] Scott Reed, Zeynep Akata, Honglak Lee, and Bernt Schiele. Learning deep representations of fine-grained visual descriptions. In *Proceedings of the IEEE conference on computer vision and pattern recognition*, pages 49–58, 2016. 2, 3
- [39] Robin Rombach, Andreas Blattmann, Dominik Lorenz, Patrick Esser, and Björn Ommer. High-resolution image synthesis with latent diffusion models. In *CVPR*, pages 10684–10695, 2022. 2
- [40] Nataniel Ruiz, Yuanzhen Li, Varun Jampani, Yael Pritch, Michael Rubinstein, and Kfir Aberman. DreamBooth: Fine Tuning Text-to-Image Diffusion Models for Subject-Driven Generation. In *CVPR*, pages 22500–22510, 2023. 5
- [41] Chitwan Saharia, William Chan, Saurabh Saxena, Lala Li, Jay Whang, Emily L Denton, Kamyar Ghasemipour, Raphael Gontijo Lopes, Burcu Karagol Ayan, Tim Salimans, et al. Photorealistic text-to-image diffusion models with deep language understanding. *Advances in neural information processing systems*, 35:36479–36494, 2022. 3
- [42] Tim Salimans, Ian Goodfellow, Wojciech Zaremba, Vicki Cheung, Alec Radford, and Xi Chen. Improved techniques for training gans. *Advances in neural information processing systems*, 29, 2016. 2
- [43] Christoph Schuhmann, Romain Beaumont, Richard Vencu, Cade W. Gordon, Ross Wightman, Mehdi Cherti, Theo Coombes, Aarush Katta, Clayton Mullis, Mitchell Wortsman, Patrick Schramowski, Srivatsa R. Kundurthy, Katherine Crowson, Ludwig Schmidt, Robert Kaczmarczyk, and Jenia Jitsev. LAION-5B: An open large-scale dataset for training next generation image-text models. In *NeurIPS*, 2022. 5
- [44] Shelly Sheynin, Adam Polyak, Uriel Singer, Yuval Kirstain, Amit Zohar, Oron Ashual, Devi Parikh, and Yaniv Taigman. Emu edit: Precise image editing via recognition and generation tasks. In *Proceedings of the IEEE/CVF Conference on Computer Vision and Pattern Recognition*, pages 8871–8879, 2024. 2, 3
- [45] Gowthami Somepalli, Anubhav Gupta, Kamal Gupta, Shramay Palta, Micah Goldblum, Jonas Geiping, Abhinav Shrivastava, and Tom Goldstein. Measuring style similarity in diffusion models. *arXiv preprint arXiv:2404.01292*, 2024. 5
- [46] StabilityAI. Stable Diffusion v2-1 Model Card, <https://huggingface.co/stabilityai/stable-diffusion-2-1>, 2022. 2
- [47] Zhenxiong Tan, Songhua Liu, Xingyi Yang, Qiaochu Xue, and Xinchao Wang. Ominicontrol: Minimal and universal control for diffusion transformer. *arXiv preprint arXiv:2411.15098*, 2024. 2, 6, 13
- [48] InstantX Team and Shaker Labs. Flux.1-dev-controlnet-union-pro. <https://huggingface.co/Shaker-Labs/FLUX.1-dev-ControlNet-Union-Pro>, 2024. 6, 13
- [49] Keyu Tian, Yi Jiang, Zehuan Yuan, Bingyue Peng, and Liwei Wang. Visual autoregressive modeling: Scalable image generation via next-scale prediction. *Advances in neural information processing systems*, 37:84839–84865, 2024. 2
- [50] Catherine Wah, Steve Branson, Peter Welinder, Pietro Perona, and Serge Belongie. The caltech-ucsd birds-200-2011 dataset. 2011. 2, 3
- [51] Peng Wang, Shuai Bai, Sinan Tan, Shijie Wang, Zhihao Fan, Jinze Bai, Keqin Chen, Xuejing Liu, Jialin Wang, Wenbin Ge, et al. Qwen2-vl: Enhancing vision-language model’s perception of the world at any resolution. *arXiv preprint arXiv:2409.12191*, 2024. 5, 14
- [52] Su Wang, Chitwan Saharia, Ceslee Montgomery, Jordi Pont-Tuset, Shai Noy, Stefano Pellegrini, Yasumasa Onoe, Sarah Laszlo, David J Fleet, Radu Soricut, et al. Imagen editor and editbench: Advancing and evaluating text-guided image inpainting. In *Proceedings of the IEEE/CVF conference on computer vision and pattern recognition*, pages 18359–18369, 2023. 3
- [53] Zhou Wang, A.C. Bovik, H.R. Sheikh, and E.P. Simoncelli. Image quality assessment: from error visibility to structural similarity. *IEEE Transactions on Image Processing*, 13(4): 600–612, 2004. 5
- [54] Shitao Xiao, Yueze Wang, Junjie Zhou, Huaying Yuan, Xingrun Xing, Ruiran Yan, Shuting Wang, Tiejun Huang, and

- Zheng Liu. Omnigen: Unified image generation. *arXiv preprint arXiv:2409.11340*, 2024. 2, 6, 13
- [55] Binxin Yang, Shuyang Gu, Bo Zhang, Ting Zhang, Xuejin Chen, Xiaoyan Sun, Dong Chen, and Fang Wen. Paint by Example: Exemplar-based Image Editing with Diffusion Models. In *CVPR*, pages 18381–18391, 2022. 2
- [56] Hu Ye, Jun Zhang, Sibor Liu, Xiao Han, and Wei Yang. Ip-adapter: Text compatible image prompt adapter for text-to-image diffusion models. *arXiv preprint arXiv:2308.06721*, 2023. 6, 13
- [57] Kai Zhang, Lingbo Mo, Wenhui Chen, Huan Sun, and Yu Su. Magicbrush: A manually annotated dataset for instruction-guided image editing. In *Advances in Neural Information Processing Systems*, 2023. 2, 3, 6, 13
- [58] Lvmin Zhang, Anyi Rao, and Maneesh Agrawala. Adding Conditional Control to Text-to-Image Diffusion Models. In *ICCV*, pages 3836–3847, 2023. 2
- [59] Shu Zhang, Xinyi Yang, Yihao Feng, Can Qin, Chia-Chih Chen, Ning Yu, Zeyuan Chen, Huan Wang, Silvio Savarese, Stefano Ermon, et al. Hive: Harnessing human feedback for instructional visual editing. In *Proceedings of the IEEE/CVF Conference on Computer Vision and Pattern Recognition*, pages 9026–9036, 2024. 3
- [60] Haozhe Zhao, Xiaojian Shawn Ma, Liang Chen, Shuzheng Si, Rujie Wu, Kaikai An, Peiyu Yu, Minjia Zhang, Qing Li, and Baobao Chang. Ultraedit: Instruction-based fine-grained image editing at scale. *Advances in Neural Information Processing Systems*, 37:3058–3093, 2024. 3, 6, 13

A. Details on Evaluation Data

Our benchmark comprises a total of 31 tasks, with each task containing between 50 and 500 evaluation cases. We provide visualizations of the conditions and exemplary generation results for each task in Fig. 7. Specifically, an evaluation case should comprise (*Introduction*, *Target Caption*, *Source Image*, *Source Mask*, *Reference Images*) to facilitate the generation and evaluation process. A detailed illustration of a complete evaluation case is presented in Tab. 1. Most of the existing image generation models support only one or a few of the 31 evaluation tasks. We provide a detailed summary of the tasks supported and unsupported by the 10 evaluated models in Tab. 2.

B. Details on Evaluation Dimensions

B.1. Aesthetic Quality



Figure 1. **Visualization of Aesthetic Quality.** Images that receive high aesthetic scores exhibit artistic appeal, whereas those with low aesthetic scores tend to appear unattractive.

Aesthetic Quality evaluates the principles of photographic composition, considering color harmony, subject arrangement, and the overall artistic impression of the image. We utilize a SigLip-based image aesthetic quality predictor to assess the aesthetic score of the generated image. The model produces a rating on a scale from 0 to 10, which we linearly normalize to a range of [0, 1] by dividing the raw score by 10.

$$S_{\text{AES}} = \frac{f_{\text{AES}}(\mathbf{I})}{10} \quad (1)$$

B.2. Imaging Quality

Imaging quality primarily examines the low-level characteristics of the generated image, such as edge sharpness, distortion, over-exposure, noise, and blur. We employ the MUSIQ image quality predictor trained on the Koniq dataset, as implemented in IQA-Pytorch [10]. For consistency and fairness in comparison, we resize the height of all generated images to 1024 pixels before inputting them into the model to assess imaging quality. This approach inherently favors high-resolution images as they typically

Table 1. **Detail of a complete evaluation case.**

| | |
|---------------------------------|--|
| <ItemID>: | b9de809c702c8cf23428ec175af3b0b9 |
| <TaskLevel1>: | Reference Editing |
| <TaskLevel2>: | Subject Reference Editing |
| <Task>: | Subject-guided Inpainting |
| <SourceImageType>: | Real Image |
| <RegionBased>: | True |
| <SourceImage>: | images/reference_editing/ subject_reference_editing/ subject_guided_inpainting/ b9de809c702c8cf234 28ec175af3b0b9_src.png |
| <SourceMask>: | images/reference_editing/ subject_reference_editing/ subject_guided_inpainting/ b9de809c702c8cf234 28ec175af3b0b9_mask.png |
| <ReferenceImages>: | ["images/reference_editing/ subject_reference_editing/ subject_guided_inpainting/ b9de809c702c8cf234 28ec175af3b0b9_ref1.png"] |
| <Instruction>: | Take <REF_1> as a reference to repaint the masked part of <SOURCE>. |
| <SourceCaption>: | Eye-level view of a street scene featuring a fire hydrant in the foreground. |
| <TargetCaption>: | A small, brightly colored toy car sits on a weathered asphalt surface, positioned slightly off-center in the foreground. The car is predominantly red and yellow, with green accents. |

exhibit superior imaging quality compared to low-resolution images. The model produces a score on a scale from 0 to 100, which we linearly normalize to a range of [0, 1] by dividing the raw score by 100.

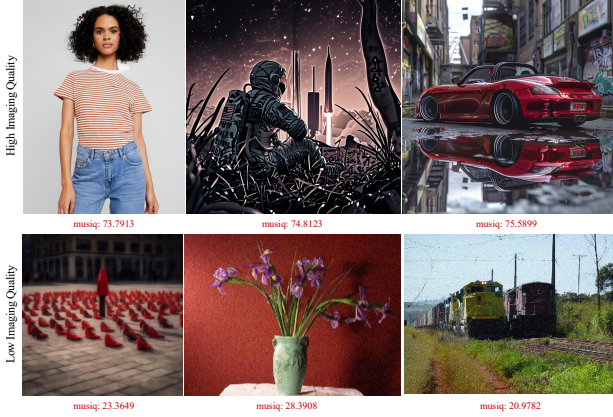
$$S_{\text{IMG}} = \frac{f_{\text{MUSIQ}}(\mathbf{I})}{100} \quad (2)$$

B.3. Prompt Following

The prompt-following score evaluates the degree to which the generated image aligns with the provided textual instructions or descriptions. For image creation tasks and controllable generation

Table 2. Task-model correspondence.

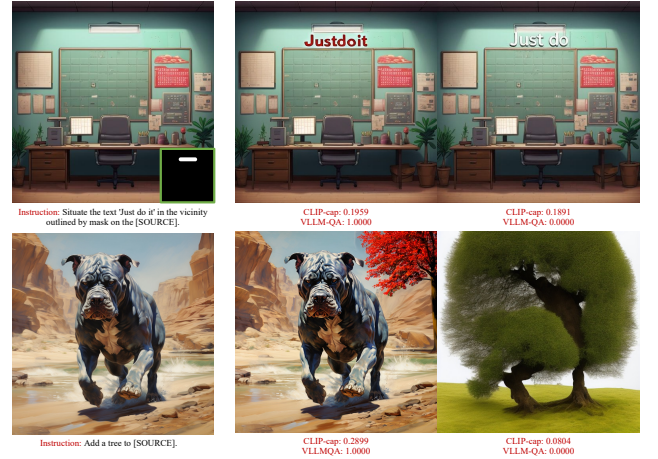
| Evaluation Tasks | | | OmniGen [54] | ACE [18] | FLUX [25] | OminiControl [47] | InstructPix2Pix [5] | MagicBrush [57] | UltraEdit [60] | FLUX-Control [48] | IP-Adapter [56] | ACE++ [29] |
|------------------|--------------|--------------------------------|--------------|----------|-----------|-------------------|---------------------|-----------------|----------------|-------------------|-----------------|------------|
| Creating | No-Ref | (1) Text-to-Image Creating | ✓ | ✓ | ✓ | × | × | × | × | × | × | × |
| | Ref | (2) Face Reference Creating | ✓ | ✓ | × | × | × | × | × | × | ✓ | × |
| | | (3) Style Reference Creating | ✓ | ✓ | × | × | × | × | × | × | ✓ | × |
| | | (4) Subject Reference Creating | ✓ | ✓ | × | ✓ | × | × | × | × | ✓ | × |
| Editing | Global | (5) Color Editing | ✓ | ✓ | × | × | ✓ | ✓ | ✓ | × | × | × |
| | | (6) Motion Editing | ✓ | ✓ | × | × | ✓ | ✓ | ✓ | × | × | × |
| | | (7) Face Editing | ✓ | ✓ | × | × | ✓ | ✓ | ✓ | × | × | × |
| | | (8) Texture Editing | ✓ | ✓ | × | × | ✓ | ✓ | ✓ | × | × | × |
| | | (9) Style Editing | ✓ | ✓ | × | × | ✓ | ✓ | ✓ | × | × | × |
| | | (10) Scene Editing | ✓ | ✓ | × | × | ✓ | ✓ | ✓ | × | × | × |
| | | (11) Subject Addition | ✓ | ✓ | × | × | ✓ | ✓ | ✓ | × | × | × |
| | | (12) Subject Removal | ✓ | ✓ | × | × | ✓ | ✓ | ✓ | × | × | × |
| | | (13) Subject Change | ✓ | ✓ | × | × | ✓ | ✓ | ✓ | × | × | × |
| | | (14) Text Render | ✓ | ✓ | × | × | ✓ | ✓ | ✓ | × | × | × |
| | | (15) Text Removal | ✓ | ✓ | × | × | ✓ | ✓ | ✓ | × | × | × |
| | | (16) Composite Editing | ✓ | ✓ | × | × | ✓ | ✓ | ✓ | × | × | × |
| | Local | (17) Inpainting | ✓ | ✓ | × | × | × | × | ✓ | × | × | ✓ |
| | | (18) Outpainting | ✓ | ✓ | × | × | × | × | × | × | × | ✓ |
| | | (19) Local Subject Addition | ✓ | ✓ | × | × | × | × | ✓ | × | × | ✓ |
| | | (20) Local Subject Removal | ✓ | ✓ | × | × | × | × | ✓ | × | × | ✓ |
| | | (21) Local Text Removal | ✓ | ✓ | × | × | × | × | ✓ | × | × | ✓ |
| | | (22) Local Text Render | ✓ | ✓ | × | × | × | × | ✓ | × | × | ✓ |
| | Controllable | (23) Pose-guided Generation | ✓ | ✓ | × | × | × | × | × | ✓ | × | × |
| | | (24) Edge-guided Generation | ✓ | ✓ | × | ✓ | × | × | × | ✓ | × | × |
| | | (25) Depth-guided Generation | ✓ | ✓ | × | ✓ | × | × | × | ✓ | × | × |
| | | (26) Image Colorization | ✓ | ✓ | × | ✓ | × | × | × | ✓ | × | × |
| | | (27) Image Deblurring | ✓ | ✓ | × | ✓ | × | × | × | ✓ | × | × |
| | Ref | (28) Style Transfer | ✓ | ✓ | × | × | × | × | × | × | × | × |
| | | (29) Subject-guided Inpainting | ✓ | ✓ | × | × | × | × | × | × | × | ✓ |
| | | (30) Virtual Try On | ✓ | ✓ | × | × | × | × | × | × | × | ✓ |
| | | (31) Face Swap | ✓ | ✓ | × | × | × | × | × | × | × | ✓ |


 Figure 2. **Visualization of Imaging Quality.** Images that achieve high imaging quality scores are typically clear and possess sharp edges, whereas those with low scores tend to appear blurry and noisy.

tasks, we compute the CLIP [36] similarity between the target caption and the generated image directly. The prompt-following score is then obtained by normalizing the CLIP similarity, specifically by dividing it by 0.5.

$$S_{PF} = \frac{\langle d_{\text{prompt}} \cdot d_I \rangle}{0.5} \quad (3)$$

Notably, for the Image Colorization and Image Deblurring tasks, CLIP similarity alone is insufficient to accurately assess prompt-following capability. For the Image Colorization task, the colorfulness score must also be considered an essential metric, leading us to adapt the prompt-following score accordingly:


 Figure 3. **Visualization of Prompt Following.** Both the CLIP-cap and VLLM-QA metrics effectively capture the successful execution of instructions.

$$S_{PF}^{\text{colorsize}} = \frac{\langle d_{\text{prompt}} \cdot d_I \rangle}{0.5} + s_{\text{color}} \quad (4)$$

In the case of the Image Deblurring task, the Imaging score serves as the prompt-following metric, as the primary objective is to enhance image quality.

$$S_{PF}^{\text{deblur}} = S_{\text{IMG}} \quad (5)$$

For image editing tasks, relying solely on CLIP similarity is insufficient to determine whether instructions have been correctly executed. To address this, we introduce a novel VLLM-based metric called VLLM-QA to assess the success of instruction align-

ment. We employ the QWEN2-VL-72B [51] model as our QA tool, prompting it with all relevant input components, including the instruction, source image, reference images, source mask, and the generated image. The model is tasked with evaluating whether the instruction has been accurately implemented; it returns a score of 1 for success and 0 otherwise. We calculate the VLLM-QA score by averaging the results across all cases within a task. Subsequently, the prompt-following score is determined as follows:

$$S_{PF} = \frac{\langle d_{\text{prompt}} \cdot d_I \rangle}{0.5} + f_{QWEN}(\cdot) \quad (6)$$

B.4. Source Consistency



Figure 4. **Visualization of Source Consistency.** Images that exhibit strong pixel alignment with the source image attain higher CLIP-src scores and lower L1 scores. These outcomes underscore the effectiveness of our evaluation of Source Consistency.

For image editing tasks, it is crucial to maintain the pixels that are unrelated to the editing instructions unchanged. To evaluate the models’ ability to preserve pixel alignment, we compute both the CLIP similarity and the mean L1 distance between the generated image and the source image. The Source Consistency score is then calculated as follows:

$$S_{SRC} = \frac{\langle d_{I_{src}} \cdot d_I \rangle + 1 - L1(I_{src}, I)}{2} \quad (7)$$

B.5. Reference Consistency

Reference consistency evaluates the semantic alignment between the reference image and the generated image across specific aspects, such as face, style, and subject. To achieve this, we utilize different encoders to extract embeddings from both the reference image and the generated image. We then assess the reference consistency in these three dimensions by calculating the feature similarity between the extracted embeddings:

$$S_{REF} = \langle d_{I_{ref}} \cdot d_I \rangle \quad (8)$$

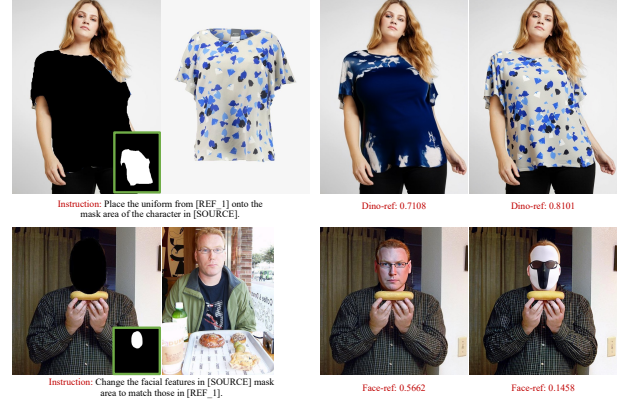


Figure 5. **Visualization of Reference Consistency.** Images that maintain identity preservation with the reference image achieve higher CLIP-ref scores, highlighting the effectiveness of our Reference Consistency evaluation.

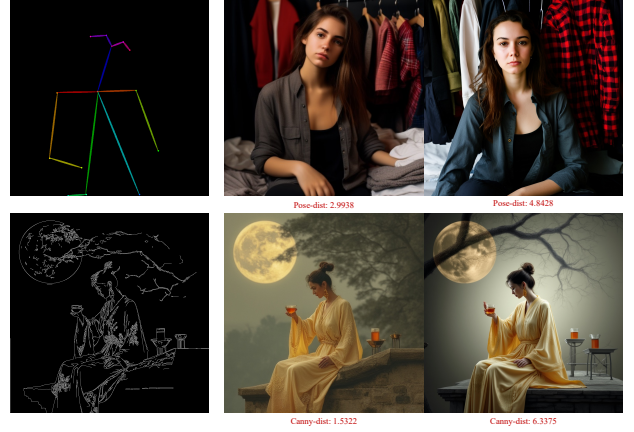


Figure 6. **Visualization of Controllability.** The Pose-dist and Canny-dist metrics effectively indicate controllability, with lower values generally signifying greater controllability.

B.6. Controllability

Controllability evaluates the alignment of low-level features in the generated image with the input condition image. For tasks such as Pose, Depth, Edge-guided Generation, and Image Colorization, we extract the relevant low-level feature map from the generated image and calculate the mean L1 score between this feature map and the input condition image. The controllability score is then determined as follows:

$$S_{CTRL} = 1 - (f_{enc}(I) - I_{src}) \quad (9)$$

While for Image Deblurring task, we employ the SSIM score as the controllability score:

$$S_{CTRL}^{deblur} = SSIM(I, I_{src}) \quad (10)$$

C. Details on Model Performance per Task

In this section, we present the detailed evaluation results for each metric across all tasks and models. The results for No-ref Image Creating are shown in Tab. 3. The results for Ref Image Creating are provided in Tab. 6. For No-ref Image Editing, the results are detailed in Tab. 4, Tab. 7, and Tab. 8. The results for Ref Image Editing are reported in Tab. 5.

Table 3. Metrics on No-ref Image Creating Task (Task 1).

| Models | Aesthetic Score↑ | Imaging Score↑ | CLIP-cap↑ |
|---------|------------------|----------------|--------------|
| ACE | 5.485 | 53.403 | 0.283 |
| OmniGen | 6.107 | 72.615 | 0.285 |
| FLUX | 6.175 | 73.480 | 0.285 |

Table 4. Metrics on Controllable Generation Tasks (Tasks 23-27).

| Task 23: Pose-guided Generation | | | | | |
|----------------------------------|------------------|----------------|--------------|--------------|--------------|
| Models | Aesthetic Score↑ | Imaging Score↑ | CLIP-cap↑ | L1-src↓ | |
| ACE | 5.568 | 50.253 | 0.299 | 0.009 | |
| OmniGen | 5.365 | 61.463 | 0.298 | 0.015 | |
| FLUX-Control | 5.538 | 56.010 | 0.298 | 0.015 | |
| Task 24: Edge-guided Generation | | | | | |
| Models | Aesthetic Score↑ | Imaging Score↑ | CLIP-cap↑ | L1-src↓ | |
| ACE | 5.319 | 49.506 | 0.298 | 0.091 | |
| OmniGen | 4.897 | 66.168 | 0.293 | 0.102 | |
| FLUX-Control | 5.493 | 54.225 | 0.296 | 0.104 | |
| OminiControl | 5.507 | 51.301 | 0.299 | 0.087 | |
| Task 25: Depth-guided Generation | | | | | |
| Models | Aesthetic Score↑ | Imaging Score↑ | CLIP-cap↑ | L1-src↓ | |
| ACE | 5.505 | 51.948 | 0.291 | 0.095 | |
| OmniGen | 4.809 | 60.266 | 0.266 | 0.131 | |
| FLUX-Control | 5.844 | 59.578 | 0.295 | 0.123 | |
| OminiControl | 5.762 | 57.305 | 0.296 | 0.098 | |
| Task 26: Image Colorization | | | | | |
| Models | Aesthetic Score↑ | Imaging Score↑ | CLIP-cap↑ | Color Score↑ | L1-src↓ |
| ACE | 5.325 | 50.484 | 0.295 | 0.278 | 0.059 |
| OmniGen | 5.275 | 61.076 | 0.289 | 0.189 | 0.185 |
| FLUX-Control | 5.371 | 51.891 | 0.302 | 0.210 | 0.067 |
| OminiControl | 5.272 | 50.995 | 0.301 | 0.161 | 0.029 |
| Task 27: Image Deblurring | | | | | |
| Models | Aesthetic Score↑ | Imaging Score↑ | SSIM↑ | | |
| ACE | 5.556 | 50.229 | 0.582 | | |
| OmniGen | 5.133 | 48.144 | 0.350 | | |
| FLUX-Control | 5.342 | 45.063 | 0.540 | | |
| OminiControl | 4.249 | 30.327 | 0.650 | | |

Table 5. Metrics on Ref Image Editing Tasks (Tasks 28-31).

| Task 28: Style Transfer | | | | | | | |
|------------------------------------|------------------|----------------|--------------|--------------|--------------|--------------|--------------|
| Models | Aesthetic Score↑ | Imaging Score↑ | CLIP -cap↑ | VLLM -QA↑ | Style -ref↑ | CLIP -src↑ | L1-src↓ |
| ACE | 5.346 | 53.030 | 0.189 | 0.323 | 0.234 | 0.762 | 0.186 |
| OmniGen | 5.045 | 62.995 | 0.193 | 0.290 | 0.359 | 0.680 | 0.277 |
| Task 29: Subject-guided Inpainting | | | | | | | |
| Models | Aesthetic Score↑ | Imaging Score↑ | CLIP -cap↑ | VLLM -QA↑ | DINO -ref↑ | CLIP -src↑ | L1-src↓ |
| ACE | 4.812 | 52.544 | 0.197 | 0.171 | 0.562 | 0.766 | 0.015 |
| OmniGen | 4.459 | 59.995 | 0.186 | 0.093 | 0.555 | 0.642 | 0.149 |
| ACE++ | 4.835 | 63.419 | 0.186 | 0.257 | 0.563 | 0.753 | 0.040 |
| Task 31: Face Swap | | | | | | | |
| Models | Aesthetic Score↑ | Imaging Score↑ | CLIP -cap↑ | VLLM -QA↑ | Face -ref↑ | CLIP -src↑ | L1-src↓ |
| ACE | 4.983 | 56.985 | 0.232 | 0.400 | 0.250 | 0.763 | 0.018 |
| OmniGen | 4.309 | 64.021 | 0.217 | 0.484 | 0.477 | 0.661 | 0.112 |
| ACE++ | 5.034 | 64.963 | 0.231 | 0.442 | 0.378 | 0.760 | 0.054 |
| Task 30: Virtual Try On | | | | | | | |
| Models | Aesthetic Score↑ | Imaging Score↑ | CLIP -cap↑ | VLLM -QA↑ | DINO -ref↑ | CLIP -src↑ | L1-src↓ |
| ACE | 4.837 | 64.723 | 0.231 | 0.629 | 0.751 | 0.889 | 0.006 |
| OmniGen | 4.696 | 73.313 | 0.235 | 0.722 | 0.744 | 0.847 | 0.058 |
| ACE++ | 4.577 | 73.525 | 0.243 | 0.804 | 0.763 | 0.882 | 0.029 |

Table 6. Metrics on Ref Image Creating Tasks (Tasks 2-4).

| Models | Task 2: Face Reference Creating | | | | Task 3: Style Reference Creating | | | | Task 4: Subject Reference Creating | | | |
|--------------|---------------------------------|--------------------------|---------------------|---------------------|----------------------------------|--------------------------|---------------------|----------------------|------------------------------------|--------------------------|---------------------|---------------------|
| | Aesthetic Score \uparrow | Imaging Score \uparrow | CLIP-cap \uparrow | Face-ref \uparrow | Aesthetic Score \uparrow | Imaging Score \uparrow | CLIP-cap \uparrow | Style-ref \uparrow | Aesthetic Score \uparrow | Imaging Score \uparrow | CLIP-cap \uparrow | DINO-ref \uparrow |
| ACE | 5.352 | 54.953 | 0.265 | 0.329 | 5.312 | 58.960 | 0.116 | 0.802 | 5.228 | 55.748 | 0.249 | 0.878 |
| OmniGen | 5.790 | 72.667 | 0.270 | 0.573 | 5.785 | 70.827 | 0.215 | 0.432 | 5.821 | 71.355 | 0.266 | 0.753 |
| IP-Adapter | 5.055 | 64.239 | 0.254 | 0.633 | 5.773 | 69.629 | 0.144 | 0.749 | 5.726 | 70.329 | 0.242 | 0.841 |
| ACE++ | 5.508 | 67.900 | 0.261 | 0.506 | - | - | - | - | 5.198 | 62.751 | 0.238 | 0.852 |
| OminiControl | - | - | - | - | - | - | - | - | 5.651 | 72.273 | 0.264 | 0.783 |

Table 7. Metrics on Global Editing Tasks (Tasks 5-16).

| Models | Task 5: Color Editing | | | | | | Task 6: Motion Editing | | | | | | Task 7: Face Editing | | | | | |
|-----------------|----------------------------|--------------------------|---------------------|--------------------|---------------------|---------------------|----------------------------|--------------------------|---------------------|--------------------|---------------------|---------------------|----------------------------|--------------------------|---------------------|--------------------|---------------------|---------------------|
| | Aesthetic Score \uparrow | Imaging Score \uparrow | CLIP-cap \uparrow | VLLM-QA \uparrow | CLIP-src \uparrow | L1-src \downarrow | Aesthetic Score \uparrow | Imaging Score \uparrow | CLIP-cap \uparrow | VLLM-QA \uparrow | CLIP-src \uparrow | L1-src \downarrow | Aesthetic Score \uparrow | Imaging Score \uparrow | CLIP-cap \uparrow | VLLM-QA \uparrow | CLIP-src \uparrow | L1-src \downarrow |
| ACE | 5.244 | 55.219 | 0.285 | 0.896 | 0.919 | 0.080 | 5.146 | 57.679 | 0.278 | 0.354 | 0.946 | 0.033 | 4.798 | 56.851 | 0.268 | 0.796 | 0.899 | 0.046 |
| OmniGen | 4.918 | 63.562 | 0.277 | 0.789 | 0.880 | 0.119 | 4.927 | 61.038 | 0.262 | 0.329 | 0.870 | 0.106 | 4.735 | 63.584 | 0.247 | 0.636 | 0.818 | 0.095 |
| InstructPix2Pix | 4.990 | 53.124 | 0.267 | 0.452 | 0.828 | 0.217 | 4.796 | 57.453 | 0.211 | 0.081 | 0.719 | 0.134 | 4.920 | 57.941 | 0.192 | 0.364 | 0.669 | 0.151 |
| MagicBrush | 4.826 | 51.677 | 0.267 | 0.604 | 0.854 | 0.094 | 4.620 | 53.121 | 0.254 | 0.267 | 0.826 | 0.081 | 4.636 | 55.833 | 0.258 | 0.660 | 0.836 | 0.054 |
| UltraEdit | 5.136 | 52.398 | 0.274 | 0.485 | 0.864 | 0.098 | 4.970 | 55.514 | 0.266 | 0.199 | 0.871 | 0.059 | 4.774 | 57.159 | 0.247 | 0.655 | 0.786 | 0.057 |
| Models | Task 8: Texture Editing | | | | | | Task 9: Style Editing | | | | | | Task 10: Scene Editing | | | | | |
| | Aesthetic Score \uparrow | Imaging Score \uparrow | CLIP-cap \uparrow | VLLM-QA \uparrow | CLIP-src \uparrow | L1-src \downarrow | Aesthetic Score \uparrow | Imaging Score \uparrow | CLIP-cap \uparrow | VLLM-QA \uparrow | CLIP-src \uparrow | L1-src \downarrow | Aesthetic Score \uparrow | Imaging Score \uparrow | CLIP-cap \uparrow | VLLM-QA \uparrow | CLIP-src \uparrow | L1-src \downarrow |
| ACE | 5.408 | 57.106 | 0.276 | 0.605 | 0.918 | 0.060 | 4.967 | 51.081 | 0.258 | 0.470 | 0.781 | 0.158 | 5.076 | 47.345 | 0.253 | 0.392 | 0.902 | 0.075 |
| OmniGen | 5.151 | 64.069 | 0.257 | 0.558 | 0.819 | 0.156 | 4.935 | 60.567 | 0.250 | 0.478 | 0.763 | 0.183 | 5.109 | 55.674 | 0.246 | 0.414 | 0.806 | 0.169 |
| InstructPix2Pix | 4.847 | 59.220 | 0.240 | 0.422 | 0.703 | 0.193 | 4.630 | 48.674 | 0.228 | 0.416 | 0.627 | 0.218 | 5.048 | 45.324 | 0.224 | 0.381 | 0.657 | 0.219 |
| MagicBrush | 4.720 | 52.909 | 0.245 | 0.463 | 0.796 | 0.122 | 4.227 | 46.647 | 0.184 | 0.140 | 0.600 | 0.249 | 4.592 | 44.262 | 0.239 | 0.464 | 0.725 | 0.189 |
| UltraEdit | 5.148 | 54.875 | 0.270 | 0.714 | 0.821 | 0.093 | 4.697 | 49.067 | 0.246 | 0.414 | 0.726 | 0.093 | 5.023 | 44.961 | 0.255 | 0.453 | 0.764 | 0.098 |
| Models | Task 11: Subject Addition | | | | | | Task 12: Subject Removal | | | | | | Task 13: Subject Change | | | | | |
| | Aesthetic Score \uparrow | Imaging Score \uparrow | CLIP-cap \uparrow | VLLM-QA \uparrow | CLIP-src \uparrow | L1-src \downarrow | Aesthetic Score \uparrow | Imaging Score \uparrow | CLIP-cap \uparrow | VLLM-QA \uparrow | CLIP-src \uparrow | L1-src \downarrow | Aesthetic Score \uparrow | Imaging Score \uparrow | CLIP-cap \uparrow | VLLM-QA \uparrow | CLIP-src \uparrow | L1-src \downarrow |
| ACE | 4.920 | 50.514 | 0.274 | 0.619 | 0.888 | 0.045 | 4.877 | 45.559 | 0.253 | 0.834 | 0.855 | 0.053 | 5.018 | 52.386 | 0.274 | 0.500 | 0.881 | 0.070 |
| OmniGen | 4.987 | 58.151 | 0.266 | 0.611 | 0.877 | 0.077 | 4.884 | 54.001 | 0.231 | 0.611 | 0.830 | 0.107 | 4.997 | 59.282 | 0.262 | 0.460 | 0.812 | 0.115 |
| InstructPix2Pix | 4.884 | 52.320 | 0.205 | 0.234 | 0.703 | 0.144 | 4.827 | 48.625 | 0.170 | 0.119 | 0.711 | 0.141 | 4.746 | 53.884 | 0.229 | 0.360 | 0.691 | 0.179 |
| MagicBrush | 4.656 | 46.127 | 0.272 | 0.594 | 0.866 | 0.061 | 4.672 | 45.197 | 0.231 | 0.322 | 0.864 | 0.069 | 4.291 | 48.950 | 0.257 | 0.500 | 0.756 | 0.123 |
| UltraEdit | 4.932 | 47.651 | 0.259 | 0.537 | 0.830 | 0.064 | 4.974 | 47.308 | 0.223 | 0.256 | 0.873 | 0.056 | 4.868 | 51.984 | 0.269 | 0.540 | 0.788 | 0.082 |
| Models | Task 14: Text Render | | | | | | Task 15: Text Removal | | | | | | Task 16: Composite Editing | | | | | |
| | Aesthetic Score \uparrow | Imaging Score \uparrow | CLIP-cap \uparrow | VLLM-QA \uparrow | CLIP-src \uparrow | L1-src \downarrow | Aesthetic Score \uparrow | Imaging Score \uparrow | CLIP-cap \uparrow | VLLM-QA \uparrow | CLIP-src \uparrow | L1-src \downarrow | Aesthetic Score \uparrow | Imaging Score \uparrow | CLIP-cap \uparrow | VLLM-QA \uparrow | CLIP-src \uparrow | L1-src \downarrow |
| ACE | 3.981 | 51.104 | 0.263 | 0.517 | 0.800 | 0.052 | 4.842 | 49.714 | 0.270 | 0.754 | 0.883 | 0.037 | 5.475 | 49.984 | 0.270 | 0.420 | 0.797 | 0.194 |
| OmniGen | 4.351 | 57.420 | 0.263 | 0.596 | 0.815 | 0.075 | 4.500 | 57.211 | 0.223 | 0.330 | 0.767 | 0.125 | 5.259 | 62.885 | 0.272 | 0.567 | 0.753 | 0.229 |
| InstructPix2Pix | 4.712 | 51.201 | 0.213 | 0.010 | 0.718 | 0.187 | 4.400 | 44.069 | 0.194 | 0.147 | 0.655 | 0.163 | 4.827 | 50.006 | 0.258 | 0.280 | 0.698 | 0.237 |
| MagicBrush | 4.458 | 45.903 | 0.261 | 0.099 | 0.845 | 0.088 | 4.359 | 44.484 | 0.260 | 0.529 | 0.838 | 0.063 | 4.665 | 47.646 | 0.245 | 0.070 | 0.732 | 0.185 |
| UltraEdit | 4.465 | 46.965 | 0.262 | 0.187 | 0.813 | 0.059 | 4.640 | 47.908 | 0.255 | 0.246 | 0.861 | 0.044 | 5.180 | 48.372 | 0.274 | 0.395 | 0.731 | 0.147 |

Table 8. Metrics on Local Editing Tasks (Tasks 17-22).

| Models | Task 17: Inpainting | | | | | | Task 18: Outpainting | | | | | | Task 19: Local Subject Addition | | | | | |
|-----------|--------------------------------|--------------------------|---------------------|--------------------|---------------------|---------------------|----------------------------|--------------------------|---------------------|--------------------|---------------------|---------------------|---------------------------------|--------------------------|---------------------|--------------------|---------------------|---------------------|
| | Aesthetic Score \uparrow | Imaging Score \uparrow | CLIP-cap \uparrow | VLLM-QA \uparrow | CLIP-src \uparrow | L1-src \downarrow | Aesthetic Score \uparrow | Imaging Score \uparrow | CLIP-cap \uparrow | VLLM-QA \uparrow | CLIP-src \uparrow | L1-src \downarrow | Aesthetic Score \uparrow | Imaging Score \uparrow | CLIP-cap \uparrow | VLLM-QA \uparrow | CLIP-src \uparrow | L1-src \downarrow |
| ACE | 4.878 | 51.793 | 0.269 | 0.833 | 0.785 | 0.024 | 5.514 | 50.403 | 0.287 | 0.376 | 0.891 | 0.017 | 4.965 | 51.704 | 0.272 | 0.555 | 0.897 | 0.029 |
| OmniGen | 4.545 | 59.264 | 0.238 | 0.524 | 0.734 | 0.108 | 5.442 | 65.758 | 0.265 | 0.326 | 0.802 | 0.114 | 4.584 | 58.911 | 0.249 | 0.479 | 0.814 | 0.066 |
| ACE++ | 5.064 | 61.661 | 0.272 | 0.910 | 0.776 | 0.016 | 5.644 | 64.156 | 0.289 | 0.531 | 0.908 | 0.010 | 5.014 | 62.083 | 0.268 | 0.785 | 0.894 | 0.018 |
| UltraEdit | 3.817 | 46.284 | 0.250 | 0.180 | 0.952 | 0.019 | 4.498 | 43.968 | 0.274 | 0.220 | 0.945 | 0.018 | 4.881 | 47.855 | 0.275 | 0.555 | 0.909 | 0.021 |
| Models | Task 20: Local Subject Removal | | | | | | Task 21: Local Text Render | | | | | | Task 22: Local Text Removal | | | | | |
| | Aesthetic Score \uparrow | Imaging Score \uparrow | CLIP-cap \uparrow | VLLM-QA \uparrow | CLIP-src \uparrow | L1-src \downarrow | Aesthetic Score \uparrow | Imaging Score \uparrow | CLIP-cap \uparrow | VLLM-QA \uparrow | CLIP-src \uparrow | L1-src \downarrow | Aesthetic Score \uparrow | Imaging Score \uparrow | CLIP-cap \uparrow | VLLM-QA \uparrow | CLIP-src \uparrow | L1-src \downarrow |
| ACE | 4.996 | 47.011 | 0.258 | 0.757 | 0.852 | 0.024 | 4.275 | 43.159 | 0.276 | 0.791 | 0.860 | 0.016 | 4.896 | 49.766 | 0.273 | 0.801 | 0.888 | 0.033 |
| OmniGen | 4.792 | 54.320 | 0.238 | 0.658 | 0.787 | 0.061 | 4.015 | 42.527 | 0.261 | 0.380 | 0.815 | 0.066 | 4.487 | 56.398 | 0.246 | 0.674 | 0.793 | 0.097 |
| ACE++ | 5.061 | 61.614 | 0.229 | 0.312 | 0.901 | 0.017 | 4.231 | 43.276 | 0.277 | 0.834 | 0.899 | 0.012 | 4.694 | 59.636 | 0.260 | 0.704 | 0.905 | 0.017 |
| UltraEdit | 4.858 | 48.748 | 0.226 | 0.287 | 0.888 | 0.018 | 4.506 | 38.887 | 0.277 | 0.098 | 0.946 | 0.014 | 4.665 | 47.294 | 0.264 | 0.714 | 0.910 | 0.023 |

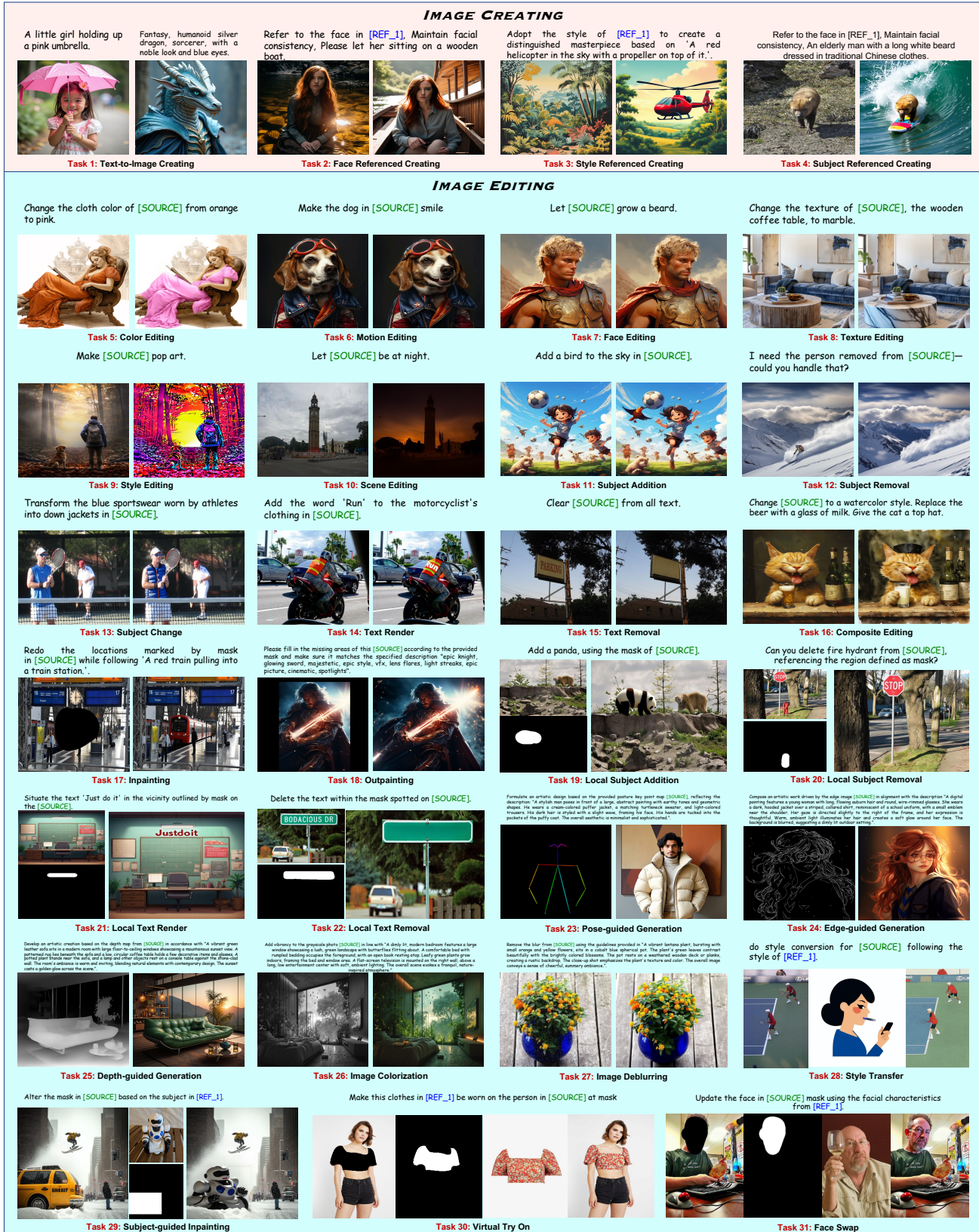


Figure 7. Examples of 31 fine-grained evaluation tasks in our ICE-Bench.